NIH Public Access
Author Manuscript
J Comp Neurol. Author manuscript; available in PMC 2007 March 20.

Published in final edited form as:
J Comp Neurol. 2006 March 20; 495(3): 299–313.

Targeting Dopamine D2 and Cannabinoid-1 (CB1) Receptors in Rat Nucleus Accumbens

VIRGINA M. PICKEL[1,*], **JANE CHAN**[1], **CHRISTOPHER S. KEARN**[2], and **KENNETH MACKIE**[2,3]

1 *Department of Neurology and Neuroscience, Weill Medical College of Cornell University, New York, New York 10021*

2 *Department of Anesthesiology, University of Washington, Seattle, Washington 98195*

3 *Department of Physiology and Biophysics, University of Washington, Seattle, Washington 98195*

Abstract

The nucleus accumbens (Acb) shell and core are essential components of neural circuitry mediating the reward and motor effects produced by activation of dopamine D2 or cannabinoid-1 (CB1) receptors. D2 receptors can form heterodimeric complexes with cannabinoid-1 (CB1) receptors and are also involved in control of the availability of both dopamine and endocannabinoids. Thus, the subcellular locations of D2 and CB1 receptors with respect to each other are implicit to their physiological actions in the Acb. We used electron microscopic immunocytochemistry to determine these locations in the Acb shell and core of rat brain. In each region, many neuronal profiles showed endomembrane and plasmalemmal distributions of one or both receptors. Approximately one-third of the labeled profiles were somata and dendrites, some of which showed overlapping subcellular distributions of D2 and CB1 immunoreactivities. The remaining labeled profiles were small axons and axon terminals containing CB1 and/or D2 receptors. Of the labeled terminals forming recognizable synapses, ~20% of those containing CB1 receptors contacted D2-labeled dendrites, while conversely, almost 15% of those containing D2 receptors contacted CB1-labeled dendrites. These results provide the first ultrastructural evidence that D2 and CB1 receptors in the Acb shell and core have subcellular distributions supporting both intracellular associations and local involvement of D2 receptors in making available endocannabinoids that are active on CB1 receptors in synaptic neurons. These distributions have direct relevance to the rewarding and euphoric as well as motor effects produced by marijuana and by addictive drugs enhancing dopamine levels in the Acb.

Keywords

marijuana; motor inhibition; reward; drug addiction; basal ganglia

The nucleus accumbens (Acb) is anatomically and functionally subdivided into several compartments, among which the medial shell and core are the most well-characterized with respect to their anatomical connectivity and function (Heimer et al., 1997; Zahm, 2000). Glutamatergic projections from the prefrontal cortex and other subcortical limbic brain regions converge with mesolimbic dopaminergic inputs to spiny neurons located in the Acb shell (Sesack and Pickel, 1990, 1992). In this region, the activation of dopamine D2 receptors can

*Correspondence to: Virginia M. Pickel, Department of Neurology and Neuroscience, Cornell University Medical College, 411 E. 69th St., Room KB-410, New York, NY 10021. E-mail: vpickel@mail.med.cornell.edu.

Grant sponsor: National Institutes of Health; Grant number: DA 04600 (to V.M.P.); Grant number: 005130 (to V.M.P.); Grant number: DA11322 (to K.M.); Grant number: DA00286 (to K.M.).

NIH-PA Author Manuscript
NIH-PA Author Manuscript
NIH-PA Author Manuscript

NIH-PA Author Manuscript

NIH-PA Author Manuscript

NIH-PA Author Manuscript

presynaptically modulate glutamate release (Kalivas and Duffy, 1997; Morari et al., 1998) in a manner that is crucial for instrumental response selection in the context of reward and psychostimulant-induced euphoria (Koch et al., 2000; van der Stelt and Di, 2003; Di Chiara et al., 2004). Cannabinoid-1 (CB1) receptors in the Acb shell are also implicated in the rewarding properties of food and many abused drugs including marijuana (Delta^9-tetrahydrocannabinol) (Gardner and Vorel, 1998; Duarte et al., 2004). The cellular mechanisms are not yet fully resolved, but may reflect CB1 receptor-mediated changes in corticostriatal transmission (Robbe et al., 2001).

The Acb core has many similarities with the dorsal striatum, which is an essential component of the basal ganglia circuitry controlling motor function (Zahm, 2000). The motor responses are evoked by glutamatergic somatosensory inputs that are potently modulated by nigrostriatal release of dopamine (Umemiya and Raymond, 1997). Moreover, the activation of striatal dopamine D2 receptors produces a time-dependent suppression of motor activity (Eilam and Szechtman, 1989). The time-dependence of this motor inhibition is comparable to that produced by activation of CB1 receptors (Romero et al., 1995), which are expressed in the dorsal striatum as well as in the shell and core of the Acb (Mailleux and Vanderhaeghen, 1992). There are also region-specific differences in the extent of the involvement of Acb D2 and CB1 receptors in sensorimotor gating and other attention-related processes (Wan and Swerdlow, 1996; Fritzsche, 2001; Geyer et al., 2001; Jongen-Relo et al., 2002). Together, these observations suggest that D2 and/or CB1 receptor systems in the Acb are essential for normal reward and motor functions, but also may play a role in psychotic disorders.

The behavioral similarities in responses obtained through activation of D2 or CB1 receptors in the Acb may largely reflect the fact that each of these receptors is coupled to inhibitory G-proteins (Bouaboula et al., 1999; Mukhopadhyay et al., 2002; Jarrahian et al., 2004; Rodriguez de Fonseca et al., 2005). Inhibition of synaptic transmission by activation of D2 or CB1 receptors is consistent with the capacity of their agonists to produce long-term synaptic depression in the Acb (Robbe et al., 2001, 2002; Ronesi and Lovinger, 2005). In contrast with the inhibition mediated through each individual receptor, D2/CB1 heterodimers are coupled to stimulatory G-proteins enhancing cyclic nucleotides in heterologous expression systems and in striatal neurons (Glass and Felder, 1997; Jarrahian et al., 2004; Kearn et al., 2005). These observations suggest that intracellular associations between D2 and CB1 receptor systems can dynamically affect the physiological actions of their endogenous and exogenous ligands. In addition, D2 or CB1 receptor activation can modulate the release of dopamine (Benoit-Marand et al., 2001; Le Foll and Goldberg, 2004), which in turn may produce a D2 receptor-mediated increase in the availability of endocannabinoids (Giuffrida et al., 2004; Centonze et al., 2004; Rodriguez de Fonseca et al., 2005). Thus, there is considerable evidence for directly or indirectly mediated functional interactions between D2 and CB1 receptor systems that could have a major impact on the output from the Acb.

Extensive coexistence of D2 and CB1 receptors in the Acb is suggested by light microscopic studies of their mRNA distributions (Hermann et al., 2002). There is, however, no ultrastructural evidence for convergent targeting of D2 and CB1 receptors in the Acb or any other brain region. In the present study, we used electron microscopic immunocytochemistry for dual labeling of antipeptide antisera against D2 and CB1 receptors in the rat Acb. The medial shell and dorsomedial core of the Acb were examined separately in order to determine the relevant sites for interactions involving these receptors in regions differentially involved in reward and motor functions. In each region, we show separate as well as coexistent and partially overlapping subcellular distributions of D2 and CB1 receptors in many neuronal profiles. The D2 receptor is also shown to be strategically positioned for involvement in the mobilization of endocannabinoids active at pre- or postsynaptic CB1 receptors.

NIH-PA Author Manuscript

NIH-PA Author Manuscript

NIH-PA Author Manuscript

MATERIALS AND METHODS

Animals

The experimental procedures were carried out in accordance with the National Institutes of Health *Guidelines for the Care and Use of Laboratory Animals*, and approved by the Institutional Animal Care and Use Committees (IACUC) at Weill Medical College of Cornell University and the University of Washington. Adult male Sprague-Dawley rats (200 –250 g; Taconic Farms, Germantown, NY) were deeply anesthetized by intraperitoneal injection of sodium pentobarbital (100 mg/kg). These animals were then either sacrificed by decapitation for rapid removal of fresh brain tissue or perfused through the ascending aorta with fixatives used for light (200 ml of 4% paraformaldehyde in 100 mM phosphate buffer (PB), pH 7.4) or electron microscopic immunocytochemistry.

The electron microscopic fixation was achieved by rapid vascular flow of 50 ml of 0.1 M PB containing 3.75% acrolein and 2% paraformaldehyde followed by 250 ml of 2% paraformaldehyde in PB. The brains were then removed from the cranium and postfixed for 30 minutes in 2% paraformaldehyde in PB. Coronal sections of 50 μm were cut through the Acb at levels 1.2–1.5 mm caudal to bregma (Paxinos and Watson, 1986) using a Leica Vibratome (Leica Microsystems, Bannockburn, IL). These sections were collected in 0.1 M PB and the acrolein-fixed tissue was then placed for 30 minutes in a solution of 1% sodium borohydride in 0.1 M PB to remove excess active aldehydes. These sections were rinsed in 0.1 M PB and placed for 15 minutes in a cryoprotectant solution (25% sucrose and 3% glycerol in 0.05 M PB) prior to freeze-thawing to enhance penetration of immunoreagents. For this, the tissue sections were frozen by sequential immersion in liquid chlorodifluoromethane (Freon, Blasco Supply, Bronx, NY) and liquid nitrogen, then thawed by immersion in 0.1 M PB at room temperature.

Antisera

A polyclonal antiserum directed towards the last 73 amino acid residues (C-terminus) of the rat CB1 receptor (Wager-Miller et al., 2002) was generated in goat. This antiserum selectively recognizes a high molecular weight (between 160 and 200 kDa) form of the receptor in Western analysis and is specific in adsorption controls using the antigenic peptide sequence (Harkany et al., 3003). This antiserum is well characterized and used previously for ultrastructural dual-labeling experiments (Pickel et al., 2004).

An antipeptide antiserum was generated in rabbit against amino acids 216 –311 of the human D2 long isoform (Brana et al., 1997), which was cloned into the pET30c plasmid (Novagen, Madison, WI) and confirmed by sequencing. This antiserum was affinity-purified and shown to be specific by positive immunolabeling in human embryonic kidney (HEK) cells transiently transfected with the pcDNA-FLAG-D2L plasmid (Kearn et al., 2005). In addition, we performed Western blots and adsorption controls to further establish the specificity of the D2 antiserum.

Rat brain membranes and Western blots were prepared with only slight modifications from those described previously for characterization of a CB1 antiserum (Wager-Miller et al., 2002). In brief, fresh brain tissue was homogenized in 10:1 volume:weight of homogenization buffer (25 mM HEPES pH 7.4, 1 mM EDTA, 6 mM $MgCl_2$, 1 mM DTT, 1 mg/ml leupeptin, 1 mg/ml pepstatin A, 1 mg/ml aprotinin). Samples were subjected to centrifugation at 700*g* for 5 minutes. The supernatants were reserved and the pellets were back-extracted in homogenization buffer. The pellets were then discarded and supernatants pooled and centrifuged at 14,000*g* for 30 minutes. The sample pellets were then washed in the original volume of homogenization buffer. The final pellets collected were resuspended, protein-

NIH-PA Author Manuscript

NIH-PA Author Manuscript

NIH-PA Author Manuscript

quantitated, and adjusted to a final concentration of 5 mg/ml in homogenization buffer. The homogenization and centrifugation procedures were done at 4°C. Each membrane sample was mixed with an equal volume of sample buffer (100 mM Tris pH 6.8, 5% β-mercaptoethanol, 4% sodium dodecyl sulfate (SDS), 20% glycerol, 0.2% bromophenol blue) and heated at 65° C for 5 minutes before loading onto 10% SDS-polyacrylamide gel. One hundred-μg samples of the membrane protein were transferred to 0.45 mm nitrocellulose (Millipore, Bedford, MA). Membranes were washed in Tris-buffered saline (TBS; 25 mM Tris, pH 8.0, 137 mM NaCl, 2.5 mM KCl). Blots were placed in a blocking buffer (LI-COR, Lincoln, NE) for 1 hour at room temperature. The blot was cut into individual strips and incubated in D2 antibody diluted 1:3,000 in a 1:1 solution of blocking buffer:TBS overnight at 4°C. Following extensive washes with TBS containing 0.05% Tween-20, the blots were incubated for 1 hour at room temperature with IR800-conjugated donkey antirabbit secondary antibody (Rockland Immunochemicals, Gilbertsville, PA). Following extensive washes in TBS-Tween, the immunocomplex was detected on the Odyssey Imaging System (LI-COR).

To prepare preadsorbed solutions used for Western blots and immunolabeling, the primary D2 antiserum at the working dilution was incubated with the D2 antigenic protein, which was coupled to Affi-Gel 10 (BioRad, Hercules, CA) for 2 hours at room temperature. For immunodetection, vibratome sections from paraformaldehyde and acrolein-fixed brains were incubated overnight at 4 – 8°C with either the affinity-purified anti-D2 antibody (1:2,000) or the adsorbed antiserum in TBS containing 0.1% Triton X-100. These were washed and processed for immunoperoxidase labeling as described below in the electron microscopic dual-labeling protocol. These sections were washed and mounted on slides for visualization of the peroxidase reaction product using a Nikon Eclipse 80i microscope (Nikon Instruments, Melville, NY). Images were captured using a Micropublisher 5.0%TV camera (QImaging, BC, Canada).

Electron microscopic dual labeling

The dual-labeling protocol used for electron microscopy was modified from that originally described by Chan et al. (1990). For this, the prepared sections from the acrolein-fixed tissue were incubated overnight at room temperature in a mixture of rabbit anti-D2 receptor antiserum (1:400 ABC; 1:250 immunogold) and goat rCB1 antiserum (1:500 ABC; 1:400 immunogold) in a solution of Tris-saline containing 0.1% bovine serum albumin (BSA).

For immunoperoxidase labeling, sections previously incubated with both primary antisera were washed and placed for 30 minutes in donkey antirabbit biotinylated immunoglobulin (IgG, 1:200) or donkey antigoat biotinylated IgG (1:200) for the respective detection of the rabbit D2 and goat CB1 antisera. These were then incubated for 30 minutes in the VectorStain ABC Elite kit (Vector Laboratories, Burlingame, CA). The product was visualized by reaction in 3,3′-diaminobenzadine (DAB, Sigma-Aldrich, St. Louis, MO) and hydrogen peroxide. Subsequently, for immunogold labeling of the second antiserum the tissue was washed and placed in a solution of Ultrasmall gold (Electron Microscopy Sciences, Hatfield, PA) conjugated to either donkey antigoat or antirabbit IgG for the respective localization of either the goat CB1 or the rabbit D2 antiserum. The particles were visualized by using the Silver IntensEM kit (Amersham, Arlington Heights, IL). The immunolabeled sections of tissue were postfixed in 2% osmium tetroxide and embedded in plastic using conventional methods (Leranth and Pickel, 1989).

Electron microscopic data analysis

The regions of the ventromedial Acb shell and dorsomedial core (plates 11–12 in the atlas of Paxinos and Watson, 1986) were chosen for ultrastructural analysis (Fig. 1). Ultrathin sections were cut from the surface of the tissue with a Leica ultramicrotome, counterstained using uranyl

NIH-PA Author Manuscript

NIH-PA Author Manuscript

NIH-PA Author Manuscript

acetate and lead citrate (Reynolds, 1963), and examined with an FEI Tecnai electron microscope. The thin sections were initially examined at low (8 –9K) magnification to identify the surface of the tissue, and those regions showing immunolabeling of both the CB1 and D2 receptors. These were then magnified and captured as digital images.

Immunoperoxidase labeling was regarded as positive when the electron-dense precipitate in individual profiles was greater than that seen in other morphologically similar profiles in the neuropil. Immunogold-labeled structures were identified as those containing one or more gold particles. This method was validated by determining in immunogold-labeled tissue the number of spurious gold-silver deposits overlying myelin and other structures not known to express either D2 or CB1 receptors. Only 2/129 myelinated axons in the D2-labeled tissue and 1/508 in the CB1-labeled material showed even one particle overlying the myelin.

Quantitative regional comparisons of the labeling patterns in Acb shell and core were done in tissue processed for dual CB1-immunogold and D2-immunoperoxidase labeling. For this, we examined thin sections that were collected equally from the surface of two vibratome sections from the Acb shell or core of four animals. In each region, electron microscopic images were obtained from an area of ~10,000 μm^2 at the tissue/plastic interface showing immunolabeling for both antisera. A more limited analysis was done in tissue processed with the reverse markers (D2-immunogold and CB1-immunoperoxidase) in which we examined thin sections from the Acb shell or core of two vibratome sections in two animals. The examined surface area in each region was ~7,000 μm^2.

In both the Acb shell and core, the structures labeled with each antiserum were separated into categories of dendrites (dendritic shafts and spines), axon terminals, small neuronal profiles (mainly unmyelinated axons and spine necks), or glial processes according to the nomenclature of Peters et al. (1991). Labeled terminals were further defined with respect to the type of synaptic specialization and presence or absence of each receptor in the postsynaptic neurons. Chi-square, analysis of variance (ANOVA), and paired *t*-test analysis was done using Statview (SAS Institute, Cary, NC) and Prism software (GraphPad Software, San Diego, CA). Microscopic illustrations were prepared by importing digital images into Adobe PhotoShop 7.0 (San Jose, CA) and Powerpoint, Microsoft Office, 2003 (Redmond, WA). The software of these programs was used to enhance contrast, prepare composite plates, and add lettering. The results are described and largely illustrated from tissue processed using immunoperoxidase for D2 and immunogold-silver for CB1 receptors. A few micrographs from tissue processed using the reverse markers are included in order to show the similarity of labeled profiles seen with each of the methods.

Figures were prepared from the acquired digital images by initial adjustment of contrast and brightness using PhotoShop 7.0 software. The same level of enhancement was applied equally to labeling seen with the adsorbed and unadsorbed antisera in Figure 1. From PhotoShop, the images were then imported into Powerpoint 2003 to add lettering and prepare the composite figures.

RESULTS

Adsorption of the D2 antiserum with the antigenic peptide sequence removed the D2 immunoreactivity in the Western blot and D2-immunolabeling in sections processed for immunocytochemistry (Fig. 1). Electron microscopic analysis of Acb shell and core regions revealed the presence of D2 and CB1 receptors in many of the same as well as separate somatodendritic and axonal profiles. The D2 and CB1 receptors showed no significant differences in their dendritic or axonal distributions in the two regions. Thus, these locations are described jointly, together with the quantitative comparisons of the Acb shell and core.

NIH-PA Author Manuscript

NIH-PA Author Manuscript

NIH-PA Author Manuscript

Dendritic distributions of D2 and CB1 receptors

Numerous dendrites and dendritic spines were immunolabeled for D2 and/or CB1 receptors. In dendritic shafts, the immunoperoxidase labeling for D2 (Fig. 2A,B) or CB1 (Fig. 2C) receptors was distributed along portions of the plasma membrane in contact with small axons and axon terminals. These terminals were variable in size and contained either all small clear or a mixture of small clear and large dense core vesicles (Fig. 2A,B). Immunogold labeling for D2 (Fig. 2C) or CB1 receptors (Fig. 2A,B,D) also was localized to surface and subsurface membranes within the larger dendritic profiles.

In dually labeled dendrites, CB1 and D2 immunoreactivities showed either separate (Fig. 2A,C), or partially overlapping (Fig. 2B,D) subcellular distributions. The overlap was seen both at the cell surface and in association with nearby endomembranes resembling smooth endoplasmic reticulum. In these locations aggregates of peroxidase reaction product were interspersed with one or more gold-silver deposits. The dually labeled portions of the dendrites were usually apposed by unlabeled axonal profiles.

In dendritic spines, CB1 (Fig. 3A) and D2 (Fig. 3B) immunoreactivities were detected near asymmetric excitatory-type synapses on spine heads. Each receptor was distributed on perisynaptic portions of the plasma membranes and beneath the postsynaptic densities at excitatory-type synapses on these dendritic spines (Fig. 3A–C). Labeling was also frequently localized to endomembranes in dendritic shafts near the base of dendritic spines (Fig. 3D,E).

Axonal distributions of D2 and/or CB1 receptors

Many small (0.1 μm) unmyelinated axons were separately labeled for D2 (Fig. 4A,B) or CB1 receptors (Fig. 4B). The axonal labeling for each of the receptors was seen either by using the highly sensitive, but diffusible immunoperoxidase method or immunogold particles. As shown for D2 (Fig. 4A) or CB1 (Fig. 4B), the peroxidase reaction product largely filled the small axons, while immunogold-silver particles had a more precise localization on the plasma membrane (Fig. 4B, for D2-immunogold). These particles were sparse, however, and only one particle was often seen in single 70 nm thin sections through axonal profiles having diameters of 0.1– 0.5 microns.

Small axons infrequently contained immunoreactivity for both D2 and CB1 receptors, although these receptors were located in apposing small axons and axon terminals (Fig. 4B–D). Other axon terminals showed single labeling for either CB1 or D2 receptors, which were also coexpressed in axon terminals. The synaptic morphology and immunolabeling in postsynaptic dendrites of the CB1- and D2-labeled terminals in the Acb shell and core are described below and summarized in Table 1.

CB1-labeled terminals and their dendritic targets—Labeling for CB1 receptors was seen in axon terminals that formed asymmetric, excitatory-type synapses with dendritic spines (Fig. 5A,B). Of the CB1-labeled terminals forming excitatory-type synapses in the Acb shell or core, ~20% were presynaptic to dendritic profiles containing D2 immunoreactivity (Fig. 5A,B), while the remainder were either unlabeled or also contained CB1 receptors (Table 1). In excitatory-type terminals containing exclusively CB1 receptors, the labeling was often located within or near the presynaptic membrane specializations (Fig. 5A,B). Dually labeled, excitatory-type terminals showed a more distal plasmalemmal and vesicular location of CB1 receptors, whose distribution partially superimposed that of D2 receptors within the same terminal (Fig. 5C). The targets of these terminals were either D2-labeled (Fig. 5C) or unlabeled dendritic spines.

NIH-PA Author Manuscript

NIH-PA Author Manuscript

NIH-PA Author Manuscript

Other CB1-labeled terminals formed symmetric inhibitory-type synapses and these synapses were located principally on dendritic shafts (Fig. 6A). In comparison with the excitatory-type terminals, CB1-labeled terminals forming inhibitory-type synapses less commonly showed postsynaptic labeling for either D2 and/or CB1 receptors (Table 1). The infrequent detection D2 receptors in these postsynaptic dendrites may, in part, reflect the sparse distribution of D2-immunogold particles within dendrites (Fig. 6A). Like the excitatory-type terminals, the CB1-labeled terminals forming symmetric synapses occasionally also contained detectable labeling for D2 receptors (Fig. 6B). The most evident overlap in the CB1 and D2 immunoreactivities in inhibitory-type terminals was seen in the perisynaptic region.

D2-labeled terminals—Axon terminals containing only D2 receptors were often small (0.2–0.3 μm) and intensely labeled (Fig. 4C). These terminals formed punctuate symmetric synapses with small dendrites and dendritic spines, but also apposed other axonal profiles converging on the same dendritic target. The apposing axon terminals were unlabeled or also contained either D2 or CB1 immunoreactivity (Fig. 4C,D).

In contrast with the smaller D2-labeled axonal profiles, larger axon terminals showed a more discrete distribution of D2 immunoreactivity on the plasma membrane and overlying synaptic vesicle membranes. The larger D2-labeled terminals often formed more clearly defined excitatory- (Fig. 4C,D) or inhibitory-type synapses. Most target dendrites were without detectable immunolabeling (Table 1). Although sparse, CB1 immunogold was seen, however, in some of the dendrites receiving input from the D2-labeled terminals (Fig. 7). These terminals included not only the larger terminals (Fig. 7A), but also smaller intensely D2-immunoreactive terminals forming punctuate symmetric synapses on dendrites showing postsynaptic plasmalemmal CB1 receptor distributions (Fig. 7B).

Regional comparison of D2 and CB1 receptors in Acb

There were no significant regional differences in numbers of single or dually labeled dendritic profiles (shafts and spines) in Acb shell and core. Specifically, the dendritic profiles comprised 46% (432/948) of all labeled structures in the Acb shell and 45% (423/937) of those in the core. Of these dendritic profiles, 34% (147/432) in the shell and 38% (162/423) in the core were immunolabeled exclusively for D2, whereas 32% (138/432) in the shell and 30% (125/423) in the core were CB1-immunoreactive. No significant shell and core differences were seen in the number of either the D2- (chi-square (1) = 1.35, $P > 0.05$) or CB1- (chi-square (1) = 0.58, $P > 0.05$) labeled dendrites. There were also no significant regional differences in the percentages of dually labeled dendritic profiles, which comprised 34% (147/432) of all labeled dendrites in the shell and 32% (136/423) of those in the core. More of the dually labeled dendrites showed overlapping cytoplasmic distributions of CB1- and D2-immunoreactivities in the core (30%, 41/136) than in the shell (21%, 31/147), but these differences also were not significant (chi-square (1) = 3.05, $P > 0.05$).

Terminals comprised 27% (258/948) of all labeled profiles in the Acb shell and 24% (223/937) of those in the core. In each region the remaining labeled neuronal processes were primarily small axons or spine necks, both of which were ~0.1 μm in diameter and not distinguishable when filled with immunoreactivity. These regional differences in labeled terminals were not significant (chi-square (1) = 2.89, $P > 0.05$). Of all labeled terminals, 37% (96/258) in the shell and 38% (85/223) in the core were exclusively labeled for D2 receptors, whereas 53% (136/258) in the shell and 52% (116/223) in the core contained only CB1 receptors. In each region the dually labeled terminals constituted ~10% of the labeled terminals (26/258, shell; 22/223).

There also was little regional variation in the numbers or types of synapses formed by CB1- or D2-labeled axon terminals in Acb shell and core. The D2-labeled terminals forming

NIH-PA Author Manuscript

NIH-PA Author Manuscript

NIH-PA Author Manuscript

excitatory-type synapses with unlabeled dendrites were, however, slightly more prevalent in the Acb shell versus core (Table 1). In each region ~30% of the CB1-labeled terminals formed synapses on dendrites containing D2 and/or CB1 receptors. Of these, the excitatory synapses with D2-containing dendrites were most commonly observed (Table 1).

DISCUSSION

These results provide ultrastructural evidence that D2 and CB1 receptors have partially overlapping subcellular distributions in both dendritic and axonal profiles of Acb shell and core. In each compartment we also observed separate locations of these receptors in neurons joined by either excitatory or inhibitory synapses (Fig. 8). These results are consistent with D2 and CB1 heterodimerization as well as involvement of D2 receptors in making available endocannabinoids active on pre- or postsynaptic CB1 receptors in the Acb. The similarities in location of D2 and CB1 receptors in the Acb shell and core suggest that the observed receptor associations are equally important for the reward and motor behaviors affected by both cannabinoids and dopamine-enhancing addictive drugs.

Methodological considerations

The CB1 and D2 antisera used in this study are well characterized and shown to specifically recognize the antigenic peptides within the C-terminal sequence of CB1 receptors (Harkany et al., 2003) or the third intracellular loop of D2 receptors, respectively (Kearn et al., 2005). Our present results extend the characterization of the D2 receptor antiserum by showing in adsorption controls that the antigenic peptide selectively removes immunoreactivity as seen by either Western blot analysis or immunocytochemical labeling in rat brain sections. The recognition of D2 and CB1 receptors, by the respective antisera, is also suggested by the similarities in their subcellular distributions to those reported previously using antisera raised against other peptide sequences of each receptor (Sesack et al., 1994; Pickel et al., 2004). We cannot, however, exclude the possibility of recognizing unknown homologous proteins, and thus all labeling should be considered as D2- and CB1-like immunoreactivity.

Individual profiles showed relatively low levels and circumscribed distributions of D2 and CB1 immunoreactivities, which often appeared as small aggregates of peroxidase reaction product or a single gold-silver deposit. Despite the scarcity of labeling, each of the markers was frequently localized to plasmalemmal or intracellular membranes that are consistent with identification of receptor proteins. In addition, each receptor had a similar subcellular location when detected with either immunogold or immunoperoxidase methods, and almost no labeling was seen over myelin or other structures expected not to contain the receptors. Together, these observations support the specificity of labeling for each receptor, but also indicate a likely underestimation of the frequencies of D2/CB1 receptor associations due to their sparse and disperse distributions in Acb neurons. This limitation would be expected to equally affect the labeling in the Acb shell and core, and thus would not influence the quantitative comparisons between the two regions.

Dendritic localization of D2 and CB1 receptors

The observed dendritic plasmalemmal distributions of D2 and CB1 receptors suggests their involvement in postsynaptic signaling in the Acb. The dendritic location of D2 receptors is consistent with evidence that these receptors are not only autoreceptors in dopaminergic terminals, but also mediators of the pre- and postsynaptic effects of dopamine in nondopaminergic striatal neurons (Jaber et al., 1996; Dani and Zhou 2004), many of which are immunolabeled for D2 receptors (Delle Donne et al., 1997). We have shown previously that CB1 receptors are also immunodetected in dendrites of both the dorsal striatum (Rodriguez et al., 2001) and Acb (Pickel et al., 2004). In the basolateral amygdala and hippocampal formation,

NIH-PA Author Manuscript

NIH-PA Author Manuscript

NIH-PA Author Manuscript

however, CB1 receptors have an almost exclusive presynaptic distribution in GABAergic terminals (Katona et al., 1999, 2001). Such regional differences may be highly relevant to specialized functions mediated through CB1 receptors in the limbic forebrain.

The observed proximity between D2 and CB1 immunoreactivities on both surface and intracellular membranes of dendrites in the Acb is consistent with observed functional associations between these receptors in striatal neurons (Glass and Felder, 1997). The Acb neurons expressing both receptors are likely GABAergic, since almost all striatal neurons contain GABA, which is coexpressed with D2 receptors in the Acb (Delle Donne et al., 1997). The striatal GABAergic neurons also contain CB1 receptor mRNA (Herkenham et al., 1991; Glass et al., 1997). Thus, the output of a subset of GABAergic neurons in the Acb may be suppressed by activation of Gi-coupled D2 or CB1 receptors (Jarrahian et al., 2004; Rodriguez de Fonseca et al., 2005). In these neurons the coactivation of each individual receptor might also result in the generation of intracellular heterodimers having opposing excitatory actions, as was recently shown in HEK 293 cells cotransfected with D2 and CB1 receptors (Kearn et al., 2005). Additional studies are needed to determine the physiological relevance of dual activation of D2 and CB1 receptors in postsynaptic Acb neurons.

D2 and/or CB1 immunoreactivities were localized to endomembranes that resemble tubulovesicular organelles that are involved in the dynamic transport of proteins in both directions along dendritic microtubules (Gruenberg et al., 1989; Prekeris et al., 1998, 1999). The identity of these membranes as portions of endomembrane systems associated with the trafficking of G-protein-coupled receptors is suggested by their resemblance to clathrin-coated pits and early endosomes, where the receptors are dephosphorylated and either retained or recycled back to the cell surface (Seachrist and Ferguson, 2003).

Differential distributions of D2 and CB1 receptors

In addition to the D2 and CB1 codistribution in dendrites and terminals (see below), these receptors also showed distinct locations in the same or separate neuronal profiles. This separation suggests that there are also important independent actions mediated through D2 and CB1 receptors in the Acb. This region contains two major subgroups of GABAergic projection neurons that are distinguishable by their content of opioid peptides (Hohmann and Herkenham, 2000). The D2 receptors are principally found in those containing proenkephalin, whereas CB1 receptors are expressed in those neurons that contain either proenkephalin or prodynorphin mRNA (Svensson and Hurd, 1998; Hohmann and Herkenham, 2000). Thus, the prodynorphin containing neurons are likely those in which cannabinoids exert their principal physiological effects through activation of D2-independent CB1 receptors. The prodynorphin containing neurons also express mu-opioid receptors (Svensson and Hurd, 1998) that are colocalized with CB1 receptors in both the dorsal striatum (Rodriguez et al., 2001) and Acb (Pickel et al., 2004). Together, these observations suggest cell-type-specific associations between D2 and CB1 receptors in the Acb as depicted in Figure 8.

Presynaptic CB1 and D2 receptors

The observed presence of CB1 receptors within the presynaptic densities of terminals forming asymmetric, excitatory-type synapses in the Acb confirms and extends our prior description of CB1 receptor location in this region (Pickel et al., 2004). In addition, we saw D2 receptor labeling in many of the dendritic targets of terminals containing CB1 receptors. Activation of D2 receptors can enhance concentrations of the endocannabinoid anandamide through both increased synthesis and decreased degradation (Centonze et al., 2004). Thus, D2 receptors in dendrites postsynaptic to excitatory-type terminals expressing CB1 receptors are ideally located for active involvement in controlling retrograde signaling through presynaptic CB1 receptors in glutamatergic terminals of the Acb (Dalia et al., 1998; Robbe et al., 2001).

NIH-PA Author Manuscript

NIH-PA Author Manuscript

NIH-PA Author Manuscript

The presynaptic CB1 receptors in excitatory-type terminals is consistent with involvement of these receptors in long-term depression of corticostriatal transmission CB1 (Robbe et al., 2001, 2002). This role is shared by D2 receptors (Stefani et al., 1995; Calabresi et al., 1997a,b) that were presently detected alone, or together with CB1 receptors, in terminals forming excitatory-type synapses on small dendrites and dendritic spines in the Acb. These terminals are likely sites for dopaminergic modulation of glutamatergic corticostriatal transmission through presynaptic D2 receptors (Morari et al., 1998; Dalia et al., 2003; Dani and Zhou, 2004). In addition, we observed appositions between D2-labeled excitatory-type terminals and smaller axonal profiles resembling striatal dopaminergic terminals (Nirenberg et al., 1997). These axonal associations suggest that the smaller terminals are sources of dopamine acting on D2 autoreceptors and heteroreceptors on the glutamatergic terminals.

Our present localization of CB1 and D2 receptors in inhibitory-type terminals in the Acb confirms and extends prior studies showing single labeling for either CB1 (Pickel et al., 2004) or D2 receptors (Delle Donne et al., 1997) in inhibitory-type terminals in this region. The activation of CB1 receptors in these terminals may modulate the release of inhibitory amino acid transmitters in the Acb, as has been shown in other striatal (Kofalvi et al., 2005) and limbic forebrain regions (Wilson et al., 2001; Szabo et al., 2002). The capacity of cocaine to inhibit, via D2-like receptors, GABA transmission is also partially prevented by CB1 antagonists, which has led to the suggestion that endocannabinoids may be downstream effectors of dopamine in the striatum (Centonze et al., 2004). The activation of each receptor may, however, independently affect the presynaptic release of inhibitory transmitters found in terminals expressing both receptors. These and other CB1-D2 receptor associations seen in the present study may be highly relevant to psychostimulant-sensitization and receptor cross-talk in the Acb.

Compartmental similarities in Acb D2 and CB1 receptor distributions

We observed no significant regional differences in the number or types of neuronal profiles containing D2 and/or CB1 receptors, and also saw no differences in the frequencies of synapses between neurons differentially labeled for these receptors. This observation was unexpected, since we have recently shown in a dual labeling study of CB1 and mu-opioid receptors that terminals containing CB1 receptors are more prevalent in the Acb shell compared with the core (Pickel et al., 2004). The differences in results obtained in the present and earlier study may largely reflect preferential sampling of regions respectively containing either D2 or mu-opioid receptors, which have distinct mRNA distributions in Acb core and shell (Curran and Watson, 1995). In contrast with the dorsal striatum, mu-opioid receptors are sparse and more homogeneously distributed in the Acb (Hurd and Herkenham, 1995), but are principally found in the dynorphin-containing neurons with extensive local collaterals in the Acb shell (Meredith et al., 2000). Thus, the greater prevalence of CB1-labeled terminals in the Acb shell in the CB1/mu dual labeling study may be largely due to more extensive sampling of the dynorphin-enriched regions. The targeting of CB1 receptors to function-specific peptidergic neurons, only some of which express D2 receptors, may contribute significantly to the diversity of cannabinoids-induced motor and affective behaviors influenced by these neuropeptides (Angulo and McEwen, 1994).

D2 receptors in the Acb, and particularly the Acb core, are critically involved in processing information related to goal-directed behaviors, including self-administration of addictive substances (Samson and Chappell, 2003, 2004). Both heroin and morphine self-administration are also affected by CB1 receptor activation (Navarro et al., 2001). Similarly, the D2 receptors in the Acb are importantly involved in disruptions in sensory gating in schizophrenia (de Bruin et al., 2001) and also affected by cannabinoids, which have psychotropic effects in humans (Stanley-Cary et al., 2002; Martin et al., 2003). Our results suggest that the convergent CB1/

NIH-PA Author Manuscript

NIH-PA Author Manuscript

NIH-PA Author Manuscript

D2 intracellular signaling and alterations in CB1 receptor activation evoked by D2 receptor mediated changes in synaptic availability of endocannabinoids are relevant to each of these important brain functions.

References

Angulo JA, McEwen BS. Molecular aspects of neuropeptide regulation and function in the corpus striatum and nucleus accumbens. Brain Res Brain Res Rev 1994;19:1–28. [PubMed: 7909470]

Benoit-Marand M, Borrelli E, Gonon F. Inhibition of dopamine release via presynaptic D2 receptors: time course and functional characteristics in vivo. J Neurosci 2001;21:9134 –9141. [PubMed: 11717346]

Bouaboula M, Bianchini L, McKenzie FR, Pouyssegur J, Casellas P. Cannabinoid receptor CB1 activates the Na+/H+ exchanger NHE-1 isoform via Gi-mediated mitogen activated protein kinase signaling transduction pathways. FEBS Lett 1999;449:61– 65. [PubMed: 10225429]

Brana C, Aubert I, Charron G, Pellevoisin C, Bloch B. Ontogeny of the striatal neurons expressing the D2 dopamine receptor in humans: an in situ hybridization and receptor-binding study. Mol Brain Res 1997;48:389 – 400. [PubMed: 9332736]

Calabresi P, Pisani A, Centonze D, Bernardi G. Synaptic plasticity and physiological interactions between dopamine and glutamate in the striatum. Neurosci Biobehav Rev 1997a;21:519 –523. [PubMed: 9195611]

Calabresi P, Pisani A, Centonze D, Bernardi G. Role of dopamine receptors in the short- and long-term regulation of corticostriatal transmission. Nihon Shinkei Seishin Yakurigaku Zasshi 1997b;17:101–104. [PubMed: 9201731]

Centonze D, Battista N, Rossi S, Mercuri NB, Finazzi-Agro A, Bernardi G, Calabresi P, Maccarrone M. A critical interaction between dopamine D2 receptors and endocannabinoids mediates the effects of cocaine on striatal GABAergic transmission. Neuropsychopharmacology 2004;29:1488 –1497. [PubMed: 15100701]

Chan J, Aoki C, Pickel VM. Optimization of differential immunogold-silver and peroxidase labeling with maintenance of ultrastructure in brain sections before plastic embedding. J Neurosci Methods 1990;33:113–127. [PubMed: 1977960]

Colombo MI, Mayorga LS, Nishimoto I, Ross EM, Stahl PD. Gs regulation of endosome fusion suggests a role for signal transduction pathways in endocytosis. J Biol Chem 1994;269:14919 –14923. [PubMed: 8195123]

Curran EJ, Watson SJ Jr. Dopamine receptor mRNA expression patterns by opioid peptide cells in the nucleus accumbens of the rat: a double in situ hybridization study. J Comp Neurol 1995;361:57–76. [PubMed: 8550882]

Dalia A, Uretsky NJ, Wallace LJ. Dopaminergic agonists administered into the nucleus accumbens: effects on extracellular glutamate and on locomotor activity. Brain Res 1998;788:111–117. [PubMed: 9554973]

Dani JA, Zhou FM. Selective dopamine filter of glutamate striatal afferents. Neuron 2004;4:522–24. [PubMed: 15157413]

de Bruin NM, Ellenbroek BA, Van Luijtelaar EL, Cools AR, Stevens KE. Hippocampal and cortical sensory gating in rats: effects of quinpirole microinjections in nucleus accumbens core and shell. Neuroscience 2001;105:169 –180. [PubMed: 11483310]

Delle Donne KT, Sesack SR, Pickel VM. Ultrastructural immunocytochemical localization of the dopamine D2 receptor within GABAergic neurons of the rat striatum. Brain Res 1997;746:239 –255. [PubMed: 9037503]

Di Chiara G, Bassareo V, Fenu S, De Luca MA, Spina L, Cadoni C, Acquas E, Carboni E, Valentini V, Lecca D. Dopamine and drug addiction: the nucleus accumbens shell connection. Neuropharmacology 2004;47(Suppl 1):227–241. [PubMed: 15464140]

Duarte C, Alonso R, Bichet N, Cohen C, Soubrie P, Thiebot MH. Blockade by the cannabinoid CB1 receptor antagonist, rimonabant (SR141716), of the potentiation by quinelorane of food-primed reinstatement of food-seeking behavior. Neuropsychopharmacology 2004;29:911–920. [PubMed: 14694354]

NIH-PA Author Manuscript

NIH-PA Author Manuscript

NIH-PA Author Manuscript

Eilam D, Szechtman H. Biphasic effect of D-2 agonist quinpirole on locomotion and movements. Eur J Pharmacol 1989;161:151–157. [PubMed: 2566488]

Fritzsche M. Are cannabinoid receptor knockout mice animal models for schizophrenia? Med Hypotheses 2001;56:638 – 643. [PubMed: 11399112]

Gardner EL, Vorel SR. Cannabinoid transmission and reward-related events. Neurobiol Dis 1998;5:502–533. [PubMed: 9974181]

Geyer MA, Krebs-Thomson K, Braff DL, Swerdlow NR. Pharmacological studies of prepulse inhibition models of sensorimotor gating deficits in schizophrenia: a decade in review. Psychopharmacology (Berl) 2001;156:117–154. [PubMed: 11549216]

Giuffrida A, Leweke FM, Gerth CW, Schreiber D, Koethe D, Faulhaber J, Klosterkotter J, Piomelli D. Cerebrospinal anandamide levels are elevated in acute schizophrenia and are inversely correlated with psychotic symptoms. Neuropsychopharmacology 2004;29:2108 –2114. [PubMed: 15354183]

Glass M, Felder CC. Concurrent stimulation of cannabinoid CB1 and dopamine D2 receptors augments cAMP accumulation in striatal neurons: evidence for a Gs linkage to the CB1 receptor. J Neurosci 1997;17:5327–5333. [PubMed: 9204917]

Glass M, Dragunow M, Faull RL. Cannabinoid receptors in the human brain: a detailed anatomical and quantitative autoradiographic study in the fetal, neonatal and adult human brain. Neuroscience 1997;77:299 –318. [PubMed: 9472392]

Gruenberg J, Griffiths G, Howell KE. Characterization of the early endosome and putative endocytic carrier vesicles in vivo and with an assay of vesicle fusion in vitro. J Cell Biol 1989;108:1301–1316. [PubMed: 2538480]

Harkany T, Hartig W, Berghuis P, Dobszay MB, Zilberter Y, Edwards RH, Mackie K, Ernfors P. Complementary distribution of type 1 cannabinoid receptors and vesicular glutamate transporter 3 in basal forebrain suggests input-specific retrograde signalling by cholinergic neurons. Eur J Neurosci 2003;18:1979 –1992. [PubMed: 14622230]

Heimer L, Alheid GF, De Olmos JS, Groenewegen HJ, Haber SN, Harlan RE, Zahm DS. The accumbens: beyond the core-shell dichotomy. J Neuropsychiatry Clin Neurosci 1997;9:354 –381. [PubMed: 9276840]

Herkenham M, Lynn AB, Johnson MR, Melvin LS, De Costa BR, Rice KC. Characterization and localization of cannabinoid receptors in rat brain: a quantitative in vitro autoradiographic study. J Neurosci 1991;11:563–583. [PubMed: 1992016]

Hermann H, Marsicano G, Lutz B. Coexpression of the cannabinoid receptor type 1 with dopamine and serotonin receptors in distinct neuronal subpopulations of the adult mouse forebrain. Neuroscience 2002;109:451– 460. [PubMed: 11823058]

Hohmann AG, Herkenham M. Localization of cannabinoid CB1 receptor mRNA in neuronal subpopulations of rat striatum: a double-label in situ hybridization study. Synapse 2000;37:71– 80. [PubMed: 10842353]

Hurd YL, Herkenham M. The human neostriatum shows compartmentalization of neuropeptide gene expression in dorsal and ventral regions: an in situ hybridization histochemical analysis. Neuroscience 1995;64:571–586. [PubMed: 7536307]

Jaber M, Robinson SW, Missale C, Caron MG. Dopamine receptors and brain function. Neuropharmacology 1996;35:1503–1519. [PubMed: 9025098]

Jarrahian A, Watts VJ, Barker EL. D2 dopamine receptors modulate Galpha-subunit coupling of the CB1 cannabinoid receptor. J Pharmacol Exp Ther 2004;308:880 – 886. [PubMed: 14634050]

Jongen-Relo AL, Kaufmann S, Feldon J. A differential involvement of the shell and core subterritories of the nucleus accumbens of rats in attentional processes. Neuroscience 2002;111:95–109. [PubMed: 11955715]

Kalivas PW, Duffy P. Dopamine regulation of extracellular glutamate in the nucleus accumbens. Brain Res 1997;761:173–177. [PubMed: 9247082]

Katona I, Sperlagh B, Sik A, Kafalvi A, Vizi ES, Mackie K, Freund TF. Presynaptically located CB1 cannabinoid receptors regulate GABA release from axon terminals of specific hippocampal interneurons. J Neurosci 1999;19:4544 – 4558. [PubMed: 10341254]

NIH-PA Author Manuscript

NIH-PA Author Manuscript

NIH-PA Author Manuscript

Katona I, Rancz EA, Acsady L, Ledent C, Mackie K, Hajos N, Freund TF. Distribution of CB1 cannabinoid receptors in the amygdala and their role in the control of GABAergic transmission. J Neurosci 2001;21:9506 –9518. [PubMed: 11717385]

Kearn CS, Blake-Palmer K, Daniel E, Mackie K, Glass M. Concurrent stimulation of cannabinoid CB1 and dopamine D2 receptors enhances heterodimer formation: a mechanism for receptor cross-talk? Mol Pharmacol 2005;67:1697–1704. [PubMed: 15710746]

Koch M, Schmid A, Schnitzler HU. Role of nucleus accumbens dopamine D1 and D2 receptors in instrumental and Pavlovian paradigms of conditioned reward. Psychopharmacology (Berl) 2000;152:67–73. [PubMed: 11041317]

Kofalvi A, Rodrigues RJ, Ledent C, Mackie K, Vizi ES, Cunha RA, Sperlagh B. Involvement of cannabinoid receptors in the regulation of neurotransmitter release in the rodent striatum: a combined immunochemical and pharmacological analysis. J Neurosci 2005;25:2874 –2884. [PubMed: 15772347]

Le Foll B, Goldberg SR. Cannabinoid CB1 antagonists as promising new medications for drug dependence. J Pharmacol Exp Ther 2004;321:875–883. [PubMed: 15525797]

Leranth, C.; Pickel, VM. Electron microscopic pre-embedding double immunostaining methods. In: Heimer, L.; Zaborszky, L., editors. Neuro-anatomical tract-tracing methods 2: recent progress. New York: Plenum; 1989. p. 129-172.

Mailleux P, Vanderhaeghen JJ. Distribution of neuronal cannabinoid receptor in the adult rat brain: a comparative receptor binding radioautography and in situ hybridization histochemistry. Neuroscience 1992;48:655– 668. [PubMed: 1376455]

Martin RS, Secchi RL, Sung E, Lemaire M, Bonhaus DW, Hedley LR, Lowe DA. Effects of cannabinoid receptor ligands on psychosis-relevant behavior models in the rat. Psychopharmacology (Berl) 2003;165:128 –135. [PubMed: 12404071]

Meredith GE, De Souza IEJ, Hyde TM, Tipper G, Wong ML, Egan MF. Persistent alterations in dendrites, spines, and dynorphinergic synapses in the nucleus accumbens shell of rats with neuroleptic-induced dyskinesias. J Neurosci 2000;20:7798 –7806. [PubMed: 11027244]

Morari M, Marti M, Sbrenna S, Fuxe K, Bianchi C, Beani L. Reciprocal dopamine-glutamate modulation of release in the basal ganglia. Neurochem Int 1998;33:383–397. [PubMed: 9874089]

Mukhopadhyay S, Shim JY, Assi AA, Norford D, Howlett AC. CB(1) cannabinoid receptor-G protein association: a possible mechanism for differential signaling. Chem Phys Lipids 2002;121:91–109. [PubMed: 12505694]

Navarro M, Carrera MR, Fratta W, Valverde O, Cossu G, Fattore L, Chowen JA, Gomez R, del Arco I, Villanua MA, Maldonado R, Koob GF, De Fonseca FR. Functional interaction between opioid and cannabinoid receptors in drug self-administration. J Neurosci 2001;21:5344 –5350. [PubMed: 11438610]

Nirenberg MJ, Chan J, Pohorille A, Vaughan RA, Uhl GR, Kuhar MJ, Pickel VM. The dopamine transporter: comparative ultrastructure of dopaminergic axons in limbic and motor compartments of the nucleus accumbens. J Neurosci 1997;17:6899 – 6907. [PubMed: 9278525]

Paxinos, G.; Watson, C. The rat brain in stereotaxic coordinates. New York: Academic Press; 1986.

Peters, A.; Palay, SL.; Webster, Hd. The fine structure of the nervous system. New York: Oxford University Press; 1991.

Pickel VM, Chan J, Kash TL, Rodriguez JJ, Mackie K. Compartment-specific localization of cannabinoid 1 (CB1) and μ-opioid receptors in rat nucleus accumbens. Neuroscience 2004;127:101–112. [PubMed: 15219673]

Prekeris R, Klumperman J, Chen YA, Scheller RH. Syntaxin 13 mediates cycling of plasma membrane proteins via tubulovesicular recycling endosomes. J Cell Biol 1998;143:957–971. [PubMed: 9817754]

Prekeris R, Foletti DL, Scheller RH. Dynamics of tubulovesicular recycling endosomes in hippocampal neurons. J Neurosci 1999;19:10324 –10337. [PubMed: 10575030]

Reynolds ES. The use of lead citrate at high pH as an electron-opaque stain in electron microscopy. J Cell Biol 1963;17:208. [PubMed: 13986422]

NIH-PA Author Manuscript

NIH-PA Author Manuscript

NIH-PA Author Manuscript

Robbe D, Alonso G, Duchamp F, Bockaert J, Manzoni OJ. Localization and mechanisms of action of cannabinoid receptors at the glutamatergic synapses of the mouse nucleus accumbens. J Neurosci 2001;21:109 –116. [PubMed: 11150326]

Robbe D, Kopf M, Remaury A, Bockaert J, Manzoni OJ. Endogenous cannabinoids mediate long-term synaptic depression in the nucleus accumbens. Proc Natl Acad Sci U S A 2002;99:8384 – 8388. [PubMed: 12060781]

Rodriguez JJ, Mackie K, Pickel VM. Ultrastructural localization of the CB1 cannabinoid receptor in mu-opioid receptor patches of the rat caudate putamen nucleus. J Neurosci 2001;21:823– 833. [PubMed: 11157068]

Rodriguez de Fonsesca F, del Arco I, Bermudez-Silva FJ, Bilbao A, Cippitelli A, Navarro M. The endocannabinoid system: physiology and pharmacology. Alcohol 2005;40:2–14.

Romero J, De Miguel R, Garcia-Palomero E, Fernandez-Ruiz JJ, Ramos JA. Time-course of the effects of anandamide, the putative endogenous cannabinoid receptor ligand, on extrapyramidal function. Brain Res 1995;694:223–232. [PubMed: 8974649]

Ronesi J, Lovinger DM. Induction of striatal long-term synaptic depression by moderate frequency activation of cortical afferents in rat. J Physiol 2005;562:245–256. [PubMed: 15498813]

Samson HH, Chappell A. Dopaminergic involvement in medial pre-frontal cortex and core of the nucleus accumbens in the regulation of ethanol self-administration: a dual-site microinjection study in the rat. Physiol Behav 2003;79:581–590. [PubMed: 12954398]

Samson HH, Chappell AM. Effects of raclopride in the core of the nucleus accumbens on ethanol seeking and consumption: the use of extinction trials to measure seeking. Alcohol Clin Exp Res 2004;28:544 –549. [PubMed: 15100604]

Seachrist JL, Ferguson SS. Regulation of G protein-coupled receptor endocytosis and trafficking by Rab GTPases. Life Sci 2003;74:225–235. [PubMed: 14607250]

Sesack SR, Pickel VM. In the rat medial nucleus accumbens, hippocampal and catecholaminergic terminals converge on spiny neurons and are in apposition to each other. Brain Res 1990;527:266 – 279. [PubMed: 1701338]

Sesack SR, Pickel VM. Prefrontal cortical efferents in the rat synapse on unlabeled neuronal targets of catecholamine terminals in the nucleus accumbens septi and on dopamine neurons in the ventral tegmental area. J Comp Neurol 1992;320:145–160. [PubMed: 1377716]

Sesack SR, Aoki C, Pickel VM. Ultrastructural localization of D2 receptor-like immunoreactivity in midbrain dopamine neurons and their striatal targets. J Neurosci 1994;14:88 –106. [PubMed: 7904306]

Stanley-Cary CC, Harris C, Martin-Iverson MT. Differing effects of the cannabinoid agonist, CP 55,940, in an alcohol or Tween 80 solvent, on prepulse inhibition of the acoustic startle reflex in the rat. Behav Pharmacol 2002;13:15–28. [PubMed: 11990716]

Stefani A, Pisani A, Bernardi G, Bonci A, Mercuri NB, Stratta F, Calabresi P. The modulation of dopamine receptors in rat striatum. J Neural Transm Suppl 1995;45:61– 66. [PubMed: 8748610]

Svensson P, Hurd YL. Specific reductions of striatal prodynorphin and D1 dopamine receptor messenger RNAs during cocaine abstinence. Mol Brain Res 1998;56:162–168. [PubMed: 9602109]

Szabo B, Siemes S, Wallmichrath I. Inhibition of GABAergic neuro-transmission in the ventral tegmental area by cannabinoids. Eur J Neurosci 2002;15:2057–2061. [PubMed: 12099913]

Umemiya M, Raymond LA. Dopaminergic modulation of excitatory postsynaptic currents in rat neostriatal neurons. J Neurophys 1997;78:1248 –1255.

van der Stelt M, Di Marzo V. The endocannabinoid system in the basal ganglia and in the mesolimbic reward system: implications for neurological and psychiatric disorders. Eur J Pharmacol 2003;480:133–150. [PubMed: 14623357]

Wager-Miller J, Westenbroek R, Mackie K. Dimerization of G protein-coupled receptors: CB1 cannabinoid receptors as an example. Chem Phys Lipids 2002;121:83– 89. [PubMed: 12505693]

Wan FJ, Swerdlow NR. Sensorimotor gating in rats is regulated by different dopamine-glutamate interactions in the nucleus accumbens core and shell subregions. Brain Res 1996;722:168 –176. [PubMed: 8813362]

Wilson RI, Kunos G, Nicoll RA. Presynaptic specificity of endocannabinoid signaling in the hippocampus. Neuron 2001;31:453– 462. [PubMed: 11516401]

Zahm DS. An integrative neuroanatomical perspective on some subcortical substrates of adaptive responding with emphasis on the nucleus accumbens. Neurosci Biobehav Rev 2000;24:85–105. [PubMed: 10654664]

NIH-PA Author Manuscript

NIH-PA Author Manuscript

NIH-PA Author Manuscript

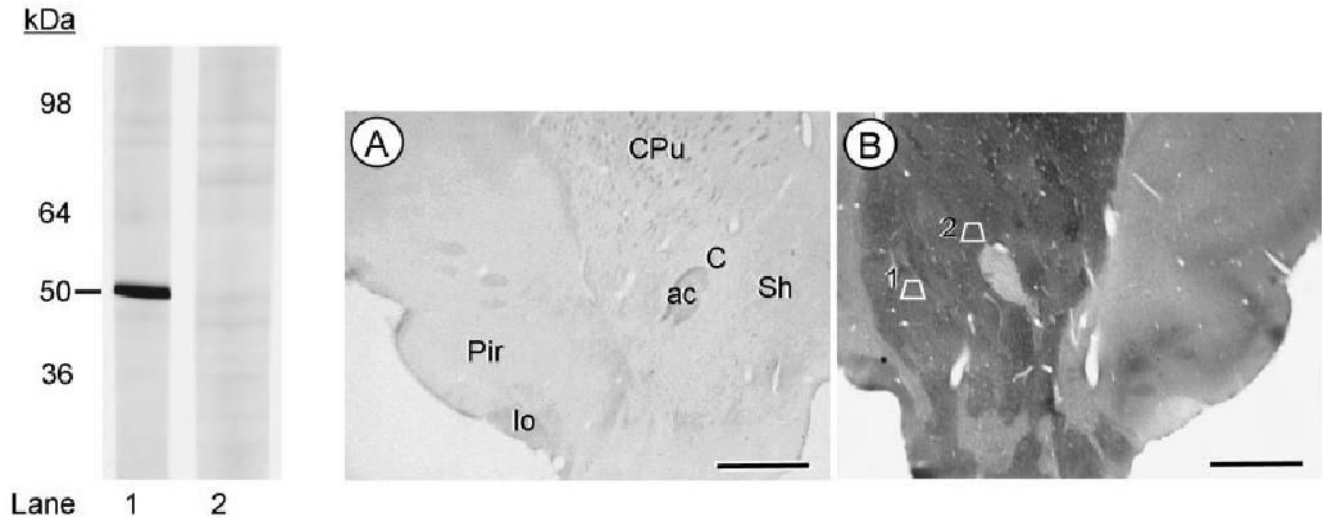

Fig. 1.

D2-antiserum characterization as seen in Western immu-noblots of rat brain membranes and immunolabeling in sections of brain tissue. In the left panel, lane 1 shows a single band at 50 kDa recognized by the D2 antiserum. In lane 2, preadsorption with immobilized antigen completely blocks detection of the D2 receptor band. Adsorption control (**A**) and immunoperoxidase labeling for the D2 antiserum (**B**) is seen in photomicrographs showing the ventral quadrant of sections through the rat brain at the level of plate 11 in the rat atlas of Paxinos and Watson (1986). The anatomical regions are identified in the control section, but equally visible in the matched section showing intense immunoperoxidase labeling in both the ventral portion of the caudate-putamen nucleus (CPu) and the nucleus accumbens core (C) and shell (Sh). Trapezoid 1 in the Acb shell and trapezoid 2 in the Acb core correspond to those regions that were sampled for electron microscopic analysis. Scale bars = 2 mm.

NIH-PA Author Manuscript NIH-PA Author Manuscript NIH-PA Author Manuscript

NIH-PA Author Manuscript
NIH-PA Author Manuscript
NIH-PA Author Manuscript

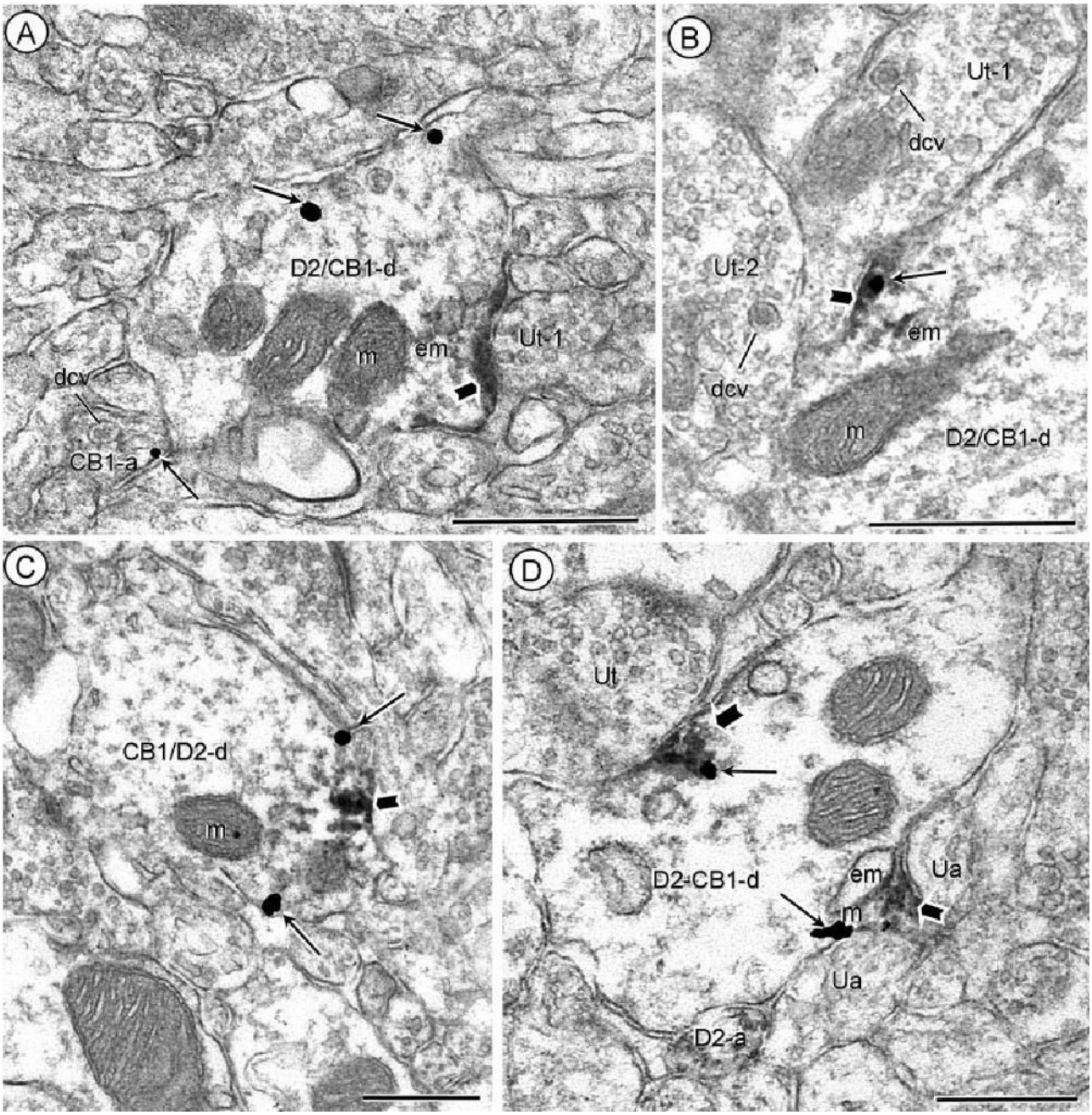

Fig. 2.

Dendritic distributions of D2 and CB1 receptors. Acb core (**A**), shell (**B**) processed for D2-peroxidase and CB1-gold immunocytochemistry. Dually labeled dendrites (D2/CB1-d) show peroxidase reaction product (block arrow) on the plasma membrane beneath unlabeled terminals (Ut-1). Gold-silver particles (small arrows) are located either distant (A) or within (B) the peroxidase aggregates at the dendritic surface. In A, gold labeling (small arrow) is also located on the plasma membrane of a nearby axon (CB1-a). Both the CB1-labeled axon in A and the unlabeled axon terminals (Ut-1 and Ut-2) in B contain numerous large dense core vesicles (dcv). **C:** Acb shell, reversal of labels, CB1-immunoperoxidase and D2-immunogold. Both the gold-silver (small arrows) and peroxidase product (block arrow) are located on or near the plasma membrane in a common dendrite (CB1/D2-d). **D:** Acb shell processed for D2-

peroxidase and CB1-gold immunocytochemistry. Aggregates of peroxidase (block arrow) and gold particles (small arrows) show overlapping distributions near endomembranes in a dually labeled dendrite (D2/CB1-d). The labeling is prevalent near regions contacted by unlabeled axons (ua) or an unlabeled terminal (Ut). Peroxidase D2-labeling is also seen in a nearby small axon (D2-a). m, mitochondria; em, endomembranes. Scale bars = 0.5 μm.

NIH-PA Author Manuscript
NIH-PA Author Manuscript
NIH-PA Author Manuscript

NIH-PA Author Manuscript
NIH-PA Author Manuscript
NIH-PA Author Manuscript

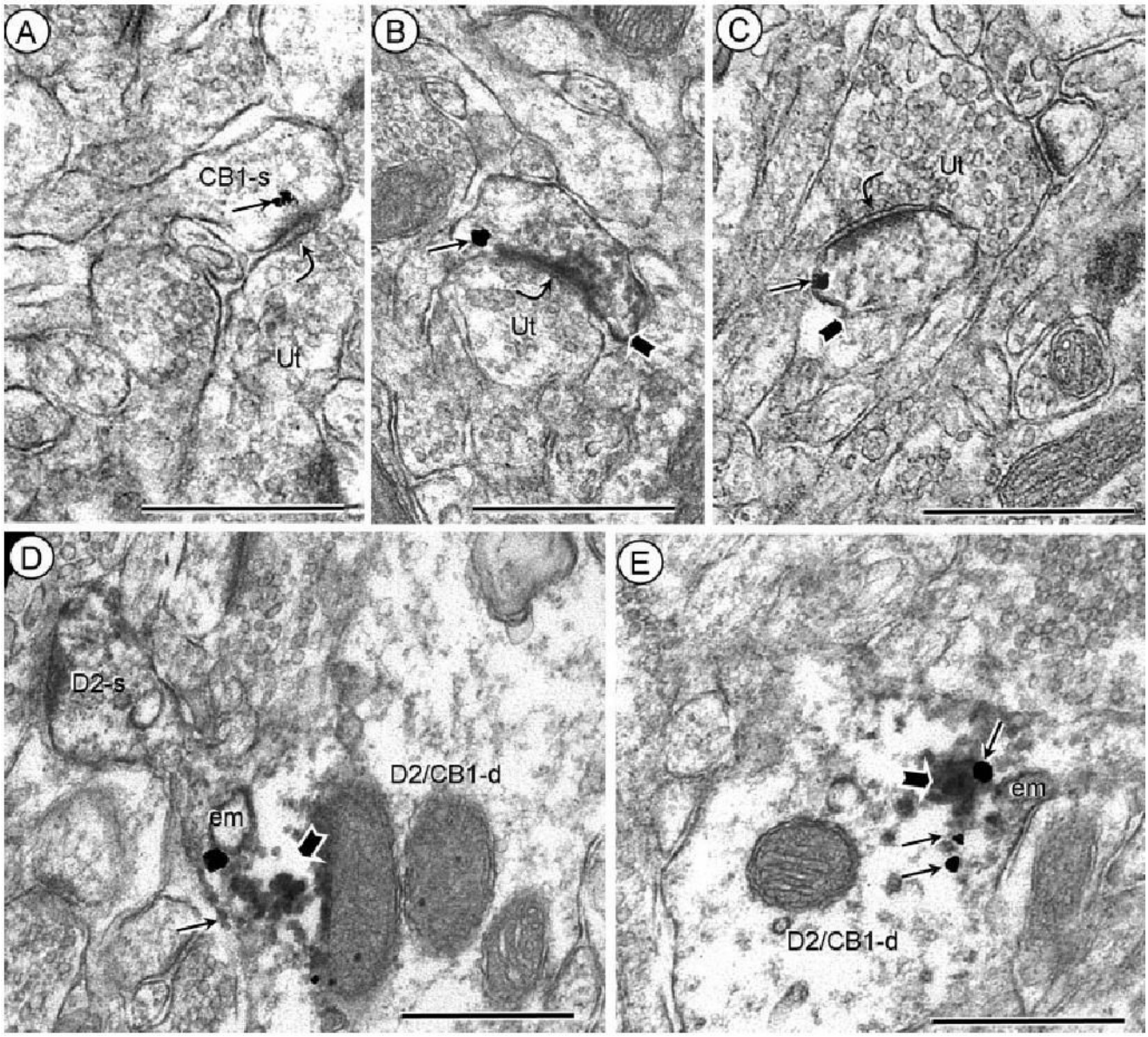

Fig. 3.

D2 and CB1 localization in dendritic spines. **A–C:** Acb core, processed for D2-peroxidase and CB1-gold immunocytochemistry. In A, CB1 gold-silver labeling (small arrows) is located in the subsynaptic region of a dendritic spine (CB1-s). In B, the peroxidase D2 labeling is diffusely distributed, but particularly evident (block arrow) along perisynaptic portions of the plasma membrane distant from the immunogold-silver CB1 labeling (small arrow) in the same dendritic spine. In C, the peroxidase (block arrow) and gold (small arrow) labeling are located in proximity to each other on the perisynaptic membrane. The spines in A–C receive asymmetric synapses (curved arrows) from unlabeled terminals (Ut). **D,E:** Acb shell, processed for D2-peroxidase and CB1-gold. Peroxidase (block arrows) and gold-silver (small arrows) show partially overlapping aggregated cytoplasmic distributions near endomembranes (em) in dually labeled den-drites (D2/CB1-d). In D, the aggregates are seen near the base of a peroxidase-labeled dendritic spine (D2-s). Scale bars = 0.5 μm.

NIH-PA Author Manuscript
NIH-PA Author Manuscript
NIH-PA Author Manuscript

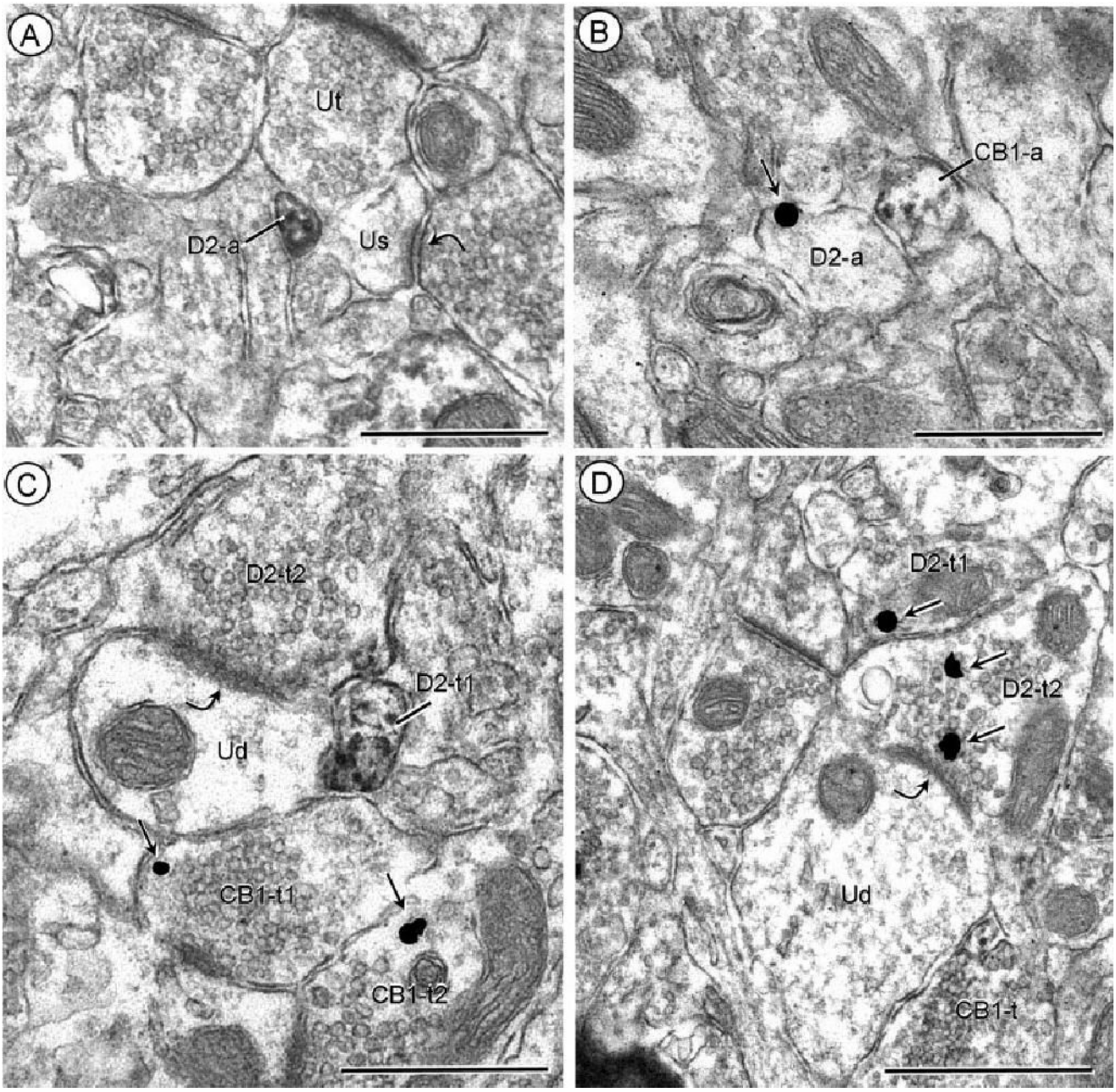

Fig. 4.

Separate localization of D2 and CB1 receptors in axonal profiles. **A:** Acb core, processed for D2-peroxidase and CB1-gold. The peroxidase reaction product is located on the plasma membrane and throughout the cytoplasm in a small unmyelinated axon (D2-a) apposing an unlabeled terminal (Ut) and an unlabeled dendritic spine (Us). This spine receives an asymmetric synapse (curved arrow) from an unlabeled axon terminal. **B:** Acb core, reverse markers with CB1-peroxidase and D2-gold. Two adjacent small axons show plasmale-mmal immunogold (small arrow; D2-a) or diffuse peroxidase reaction product (CB1-a). **C:** Acb shell, processed for D2-peroxidase and CB1-gold. D2 immunoreactivity is distributed throughout a small preter-minal axonal process (D2-t1) and on the apposed plasma membrane and subsurface vesicles within a large terminal (D2-t2), which forms an asymmetric synapse

NIH-PA Author Manuscript

NIH-PA Author Manuscript

NIH-PA Author Manuscript

(curved arrow) with an unlabeled dendrite (Ud). A convergent terminal (CB1-t1) on the same dendrite and another terminal (CB1-t2) within the neuropil contain isolated immu-nogold particles (small arrows) indicating the presence of CB1 receptors. **D:** Acb shell, with reversal of markers, CB1 peroxidase and D2-gold. Immunogold (small arrows) labeling is seen in two apposed terminals (D2-t1 and t2), the latter of which forms what appears to be a tangentially sectioned asymmetric synapse (curved arrow) with an unlabeled dendrite (Ud). The dendrite is apposed by an axon terminal showing diffuse CB1-immunoperoxidase labeling (CB1-t). Scale bars = 0.5 μm.

NIH-PA Author Manuscript
NIH-PA Author Manuscript
NIH-PA Author Manuscript

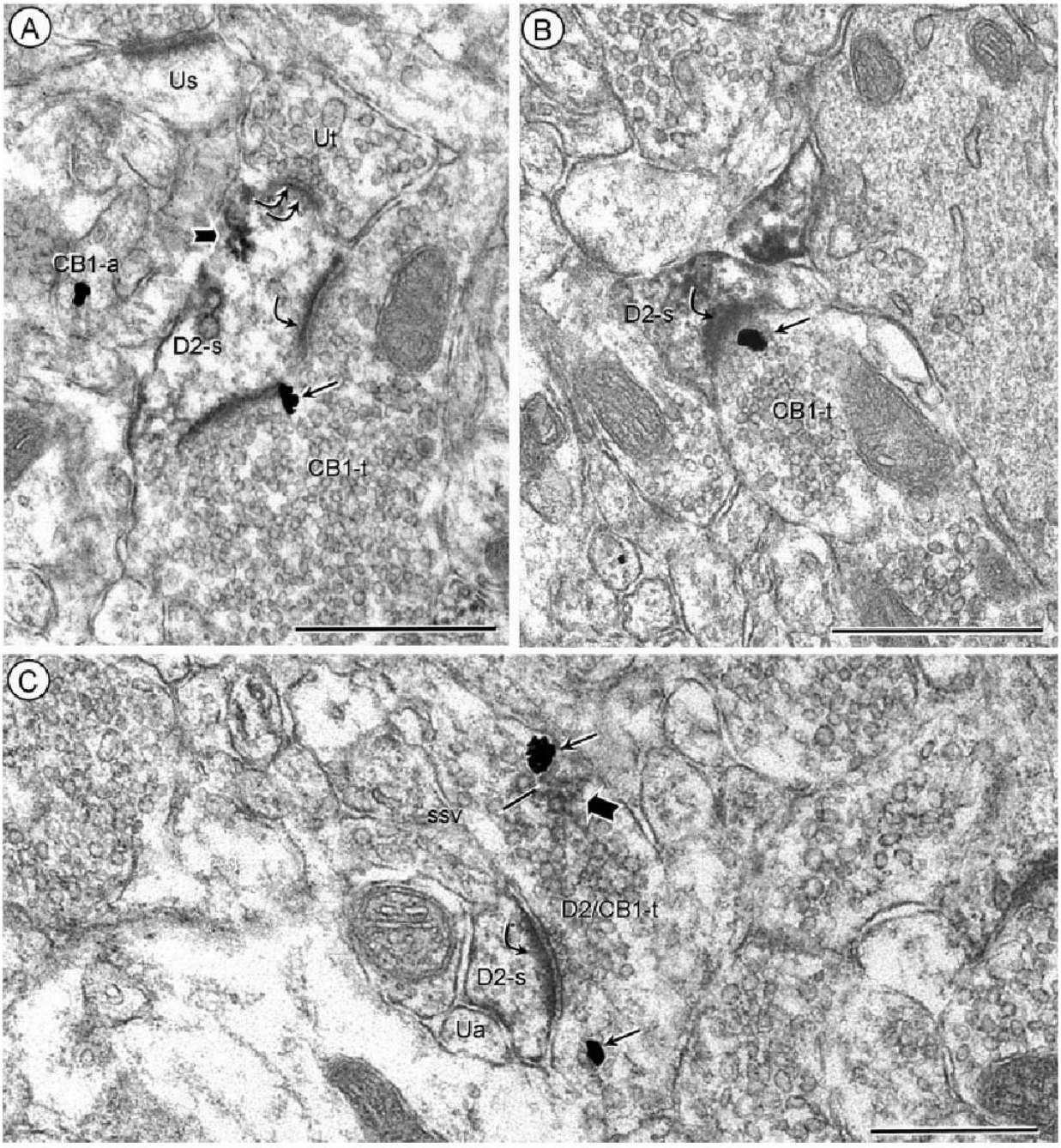

Fig. 5.

CB1 and D2 distributions in axon terminals forming excitatory-type synapses with D2-labeled dendritic spines. Acb core (**A**), and Acb shell (**B**) processed for D2-peroxidase and CB1-gold. Immunogold CB1 labeling (small arrows) is located on the presynaptic plasma membrane of an axon terminal (CB1-t) forming an asymmetric synapse (single curved arrow) with a dendritic spine showing peroxidase reaction product (block arrows) for the D2 receptor (D2-s). The dendrite in A is also contacted (double curved arrow) by an unlabeled terminal (Ut). **C:** Acb core, processed using the same immunolabels as in A and B. The peroxidase reaction product and immunogold are colocalized in an axon terminal (D2/CB1-t) forming an asymmetric synapse (curved arrow) with a D2-immunoperoxidase labeled spine (D2-s). Within the dually

NIH-PA Author Manuscript

NIH-PA Author Manuscript

NIH-PA Author Manuscript

labeled terminal, each marker is distributed away from the presynaptic plasma membrane and in association with small synaptic vesicles (ssv). The spine is apposed by a small unlabeled axon (Ua). Scale bars = 0.5 μm.

NIH-PA Author Manuscript
NIH-PA Author Manuscript
NIH-PA Author Manuscript

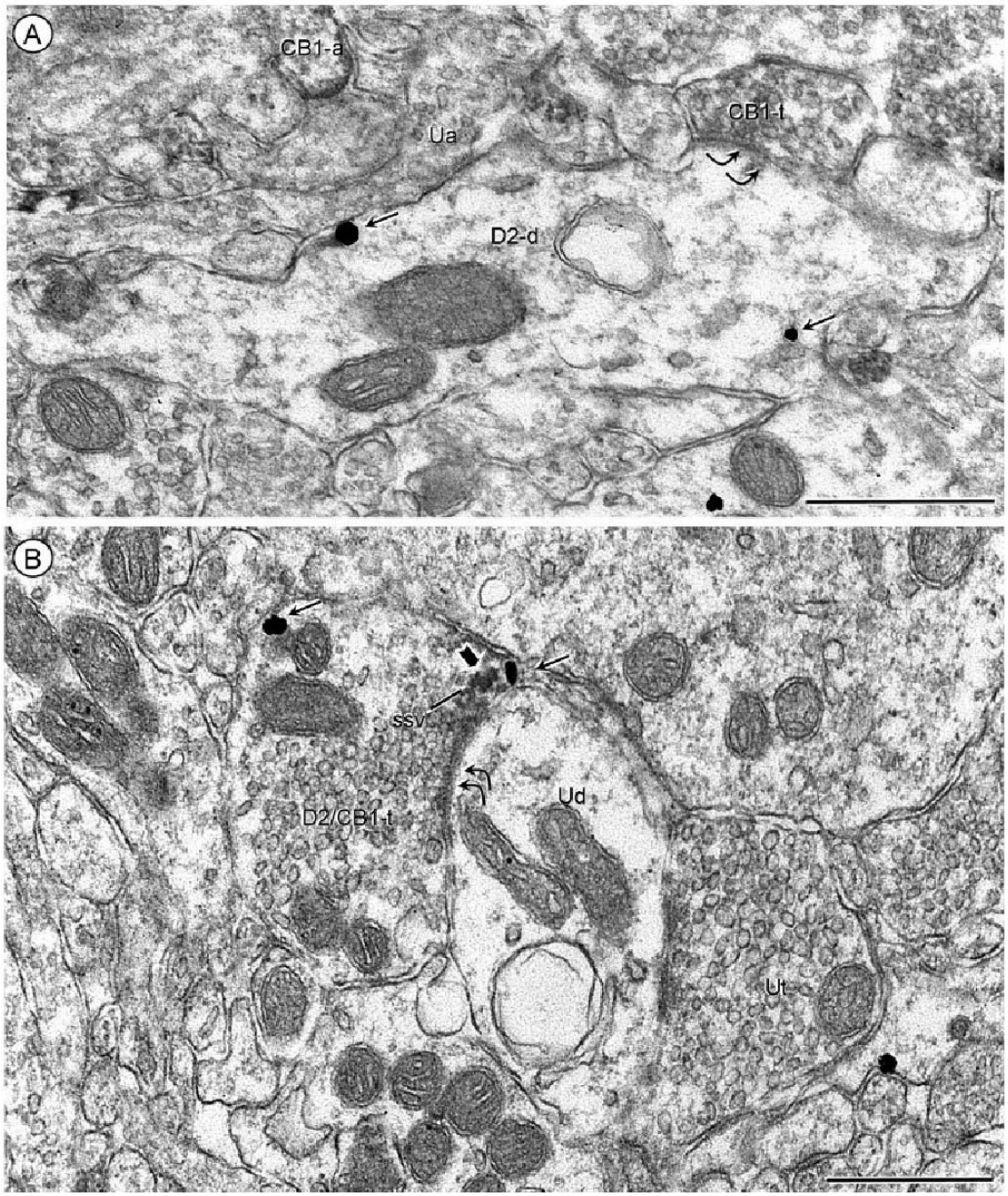

Fig. 6.

CB1 receptor location in inhibitory-type terminals. **A:** Acb core, processed for CB1 immunoperoxidase and D2 immunogold labeling. The peroxidase CB1 reaction product is diffusely distributed in an axon terminal (CB1-t) that forms a symmetric synapse (double curved arrows) with a dendrite containing D2 immunogold (small arrows). **B:** Acb shell, processed for D2-peroxidase and CB1-gold. The peroxidase reaction product (block arrow) and immunogold (thin arrows) have partially overlapping presynaptic distributions in a dually labeled axon terminal that forms a symmetric synapse with an unlabeled dendrite (Ud). Scale bars = 0.5 μm.

NIH-PA Author Manuscript
NIH-PA Author Manuscript
NIH-PA Author Manuscript

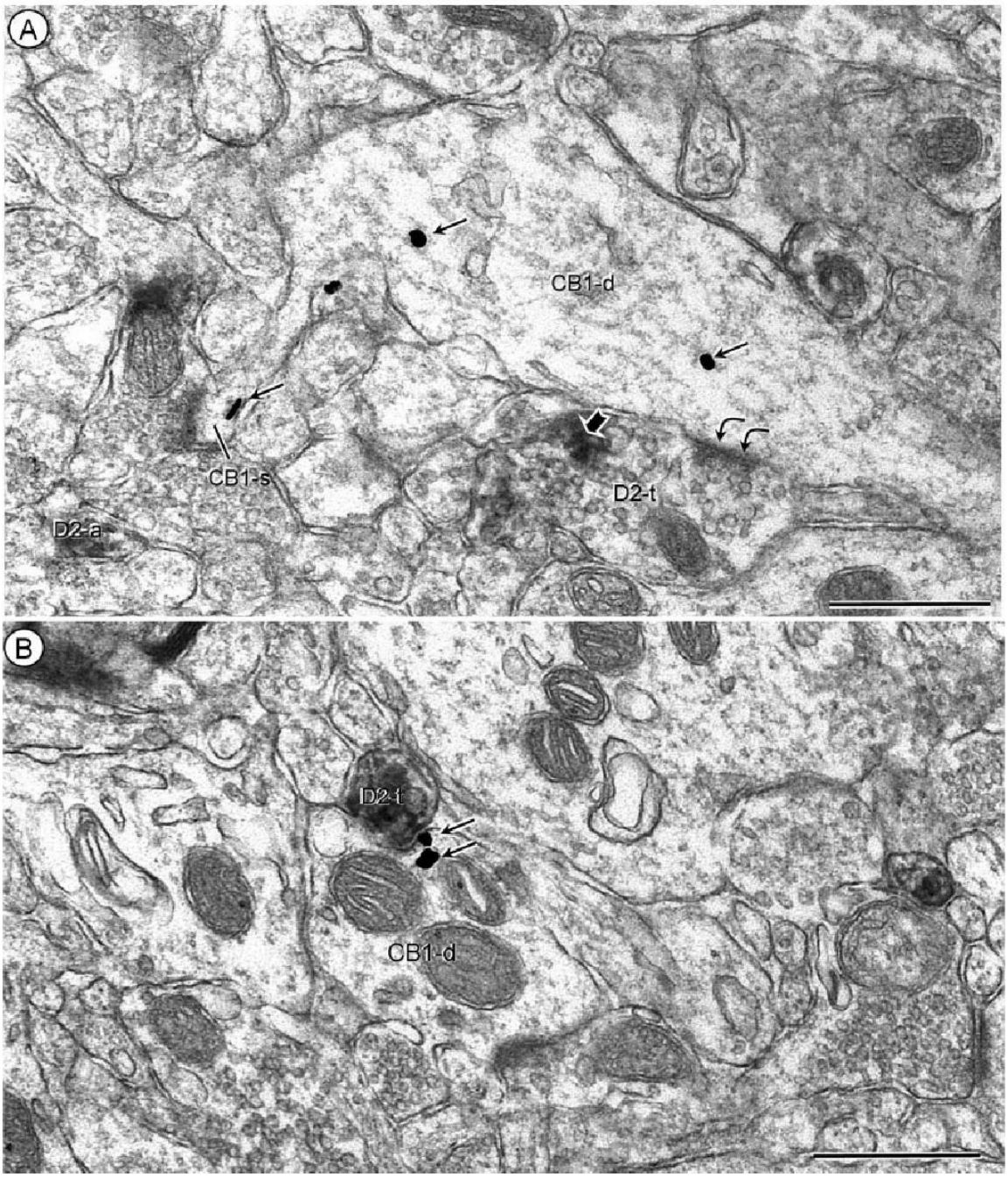

Fig. 7.

Localization of D2 receptors in terminals presynaptic to CB1-labeled dendrites. **A:** Acb core, processed for D2-peroxidase and CB1-gold. D2 receptor immunoperoxidase (block arrow) is present in an axon terminal (D2-t) forming a symmetric synapse (double curved arrows) with a dendrite that shows CB1 immunogold (thin arrows) in both the dendritic shaft (CB1-d) and spine (CB1-s). **B:** Acb shell, processed for D2-peroxidase and CB1-gold. Peroxidase immunoreactivity is seen throughout a small terminal (D2-t) forming a punctuate synapse with a dendrite (CB1-d) in which the CB1 immunogold-silver particles (small arrows) are located within and near the synapse. Scale bars = 0.5 μm.

NIH-PA Author Manuscript
NIH-PA Author Manuscript
NIH-PA Author Manuscript

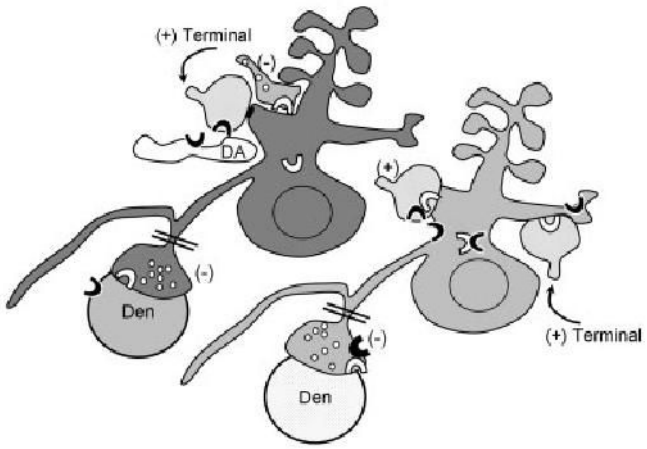

Fig. 8.

Schematic diagram showing co-expression and partially intracellular distributions of CB1 (white block arc) and D2 (black block arc) in a spiny neuron (light gray shading), whose local inhibitory (−) terminal also contains both markers. An adjacent spiny neuron (dark gray) expresses CB1 (white block arc), but not D2 receptors. Putative dopaminergic (DA) and apposed excitatory (+) type terminals, both containing D2 receptors, are presynaptic to the dendrite that contains CB1 receptor. Conversely, the dendritic profiles (light gray shading) labeled for D2 receptors including those that also contain CB1 receptors are postsynaptic to CB1- or CB1- and D2-labeled excitatory inputs (+). Inhibitory-type (−) terminals, likely originating as collaterals of the spiny projection neurons (double bar), are immunolabeled for either CB1 or CB1 and D2. These are shown as presyn-aptic to dendrites (Den) that are unlabeled (white stipple) or labeled for the D2 receptor.

NIH-PA Author Manuscript

NIH-PA Author Manuscript

NIH-PA Author Manuscript

TABLE 1

Percentage of CB1 and D2 Terminals in Acb Shell and Core Forming Subtype-Selective Synapses With Differentially Labeled Dendritic Targets

Acb region	Terminal labeling	Synaptic subtype	Immunolabeling in postsynaptic targets			
			None	D2	CB1	D2/CB1
Shell	CB1	Excitatory	44.8	20.7	6.9	0.0
	N = 87*	Inhibitory	13.8	2.3	4.6	6.9
Core	CB1	Excitatory	42.7	20.6	3.7	2.4
	N = 82	Inhibitory	17.1	4.9	4.9	3.7
Shell	D2	Excitatory	56.5	8.7	4.3	0.0
	N = 42	Inhibitory	19.6	0.0	8.7	2.2
Core	D2	Excitatory	30.6	11.1	8.3	5.6
	N = 36	Inhibitory	19.4	5.6	13.8	5.6

* Number of synaptic CB1 or D2 labeled terminals in an area of approximately 10,000 μm^2 in each Acb region from two sections in four rats. Tissue was processed using immunogold for CB1 and immunoperoxidase for D2 receptors.